

DETERMINATION OF FRAME FOR TSUNAMI CAPSULE PASSENGERS BASED ON THE RESULTS OF STRESS AND STRAIN USING OCTAHEDRAL DISCRETIZATION

Mochamad Edoward Ramadhan^{1,*}, Gaguk Djatisoekamto¹

¹Mechanical Engineering Department, Faculty of Engineering, University of Jember
Jl. Kalimantan No.37, 68121, Jember, East Java

*E-mail: edoward.teknik@unej.ac.id

Accepted: 26-11-2019

Revised: 29-05-2020

Approved: 01-06-2020

ABSTRACT

The prototype research for the safety capsule began with the tsunami that struck Indonesia as an archipelago. Besides, the United States, Japan, and China have made successful tsunami capsules in patent RIGHTS with the code US4297757 (America) spherical and in China, there are about 5 shapes that have been made CN102267549B (mushroom forms); CN203698627U (cup shape); CN204750532U (bunker form); CN204916125U (cylindrical capsule form); CN208198781U (ovoid shape). After examining existing patents and prototypes, the researchers made a prototype in the shape of a ball with a diameter of 2 meters. The material uses Stainless steel outer diameter of 25.4mm and an inner diameter of 23.9mm. The simulation uses octahedral discretion by mesh adjusting to the structure. The load uses pressure in the outer surface area, a person load of 4 with a weight of 60kg each, and for fixed constraints on the inside of spherical geometry. The purpose of the simulation is to predict the location of critical areas that experience the greatest stress and strain. The concept is applied based on the number of amplifiers given in the form of a square as a reference, the concept of 1 amplifier is given a vertical direction, the concept of 2 vertical and horizontal directions, the concept of 3 diagonal crosswise, the concept of 4 diagonal crosses and 1 amplifier of the vertical direction, the concept of 5 diagonal crosses and the direction horizontal vertical, the concept of 6 square in the middle with vertical and horizontal amplifiers, the concept of 7 square in the middle with the diagonal crossing amplifier, the concept of 8 triangles in the middle with the bottom diagonal in the middle and one horizontal direction, the concept of 9 triangles in the middle with crossed diagonals and added a directional line horizontally, the concept of 10 hexagons with the edges is given an amplifier up to the frame. The results of the simulation selection, concept 3, and Concept 6 have a strain of 0.00725 mm, while Concept 6 has principal stress smaller than Concept 3 which is 3.05×10^6 N/m with an estimated local error of 2.13×10^{-6} Joules. So that Concept 6 is set to be used as an amplifier of prototype tsunami safety capsules.

Keywords: Stress; Strain; Octahedral; Critical Area; Tsunami Capsules.

1. INTRODUCTION

The making of a framework of a safety capsule prototype as an effort in response to natural disasters for the people of Indonesia is a very important requirement. The prototype consists of parts, framework, interior, and

exterior. Part of the framework with various shapes is freedom for the makers, on this occasion, the researchers will make a prototype with a 2000 mm diameter ball shape. The framework is made of steel pipes with an inner diameter of 23.9 mm and an outer diameter of 25.4 mm, while loading uses pressure loads for

the outermost ball frame and the inside is fixed with a load of 60 kg. Because the inside is connected to the seat of a person, the load is given vertically down and some horizontally for the placement point of the passenger belt. Meshing uses the adaptive discretion of octahedral elements. Finite Element Analysis is used to determine the critical area of the prototype, after which it is given an amplifier in the form of a frame. The frame also developed 10 concept concepts and Finished Element Method Analysis was carried out to determine the frame concept to be applied using the 6th concept.

2. METHODS

2.1. Finite Element Method (FEM)

Finite Element Method (FEM), which aims to approach the method by dividing a geometry into finite small parts (discretization). The word "finite or finite" means that the process of discretization is not infinite, with the completion of the integral analysis method. FEM is defined as a numerical approach to solving geometric problems expressed in differential equations [1]. FEM can be done in the following steps:

- a. Draw geometric shapes in 3 dimensions,
- b. Meshing using nursing elements,
- c. Load and support,
- d. Run the Simulation and get the stress and strain results in FEM.

The simple simulation that applies to each element. For example, in simulating a spring, FEM is used to find the amount of stress directly proportional to its shape change by creating a simple formula for each of these elements. The following is the mathematical formulation of physics from Spring stiffness:

$$F_{spring} = k \cdot x \quad (1)$$

k = spring strength constant,
x = change in spring length.

5. Entering all data elements needed to support FEM resolution which is often called the initial conditions. [3] In geometry, an octahedron is a polyhedron with eight surfaces, twelve edges, and six vertices. The subject is well known and is used to use ordinary octahedron elements,

Platonic solids consisting of eight equilateral triangles, four of which meet at each point can be seen in figure 1. Regular Octahedrons are double cube polyhedrons. This is a fixed tetrahedron. Square bipyramid in one of three orthogonal orientations. It is a triangular antiprism in one of four orientations. If there is a field that experiences a force in the form of pressure or pulls then the field experiences stress. Based on the technical dictionary that stress is divided into engineering stress and the true stress. The application of stress in everyday life, the force has units of pounds or newtons, while the area of contact has units of inch² or mm². So the stress is the amount of the derivative expressed in pounds/in² (1 psi) or N/mm² (1 MPa) [2]. The amount of stress depending on the style given. In use, the word stress has the meaning: The force in units of area or stress intensity is defined as the unit stress. The force in the amount of a single rod which is generally said to be the overall stress when the object receives a load of P in kg, causing the object to grow longer or shorter by ΔL mm followed by an increase in the narrow or cross-sectional area of the object being subjected to pull and pressure. In conditions like the one above, the deadline can be calculated using the following formula (engineering stress):

$$\sigma = F/A_0 \quad (2)$$

σ = stress (pascal, N/m²),
F = apply loads (Newton, dyne)
A₀ = initial cross-sectional area (mm²).

While true stress is the stress obtained from the measurement of the intensity of the reaction force (from force measuring devices) divided by the surface area (the measurement of the area of contact force on the field) under actual conditions. True stress can be calculated by:

$$\sigma = F/A \quad (3)$$

σ = True stress (MPa),
F = Apply Loads (N),
A = Initial cross-sectional area (mm²).

A strain is defined as a change in the length of the material due to the force divided by the initial length before applying the compressive or tensile force to the material. The elasticity limit (the ability of the material to return to its original form after being exerted force and removed) has a strain and stress ratio by forming

a linear equation and will end up at the point of stretching and eventually experience a material failure or breakage. The relationship between stress and strain becomes non-linear when the material reaches the plastic area. Strain due to the stress experienced by an object can be divided into two, namely: engineering strain and true strain. Engineering strain is a strain that uses mathematical equations based on changes in the dimensions of the original object (initial length), to determine the value of the magnitude of the strain that occurs by dividing the extension or shortening with the original length by:

$$\text{Elong} = (L_a - L_o) / L_o = \Delta L / L_o \quad (4)$$

ΔL = Change in length,

L_o = Initial length,

L = Length after being applied in load.

True strains can be calculated in stages (increment strains), the amount of strain is calculated on the condition of the dimensions of objects when experiencing stress (actually) and not calculated based on the initial length of dimensions of objects when not experiencing stress. The strain equation for true strain (ϵ) is:

$$\epsilon = (L_a - L_o) / L_a \quad (5)$$

Deformation occurs when an object is given a force of view of the object will absorb energy as a result of the force acting. Physical shape changes due to divided into two, namely plastic deformation and elastic deformation. Giving a load on an object with material that can withstand the highest strength cannot be done, so it can be done that the object undergoes total deformation. If a load is used in an object, then the strain will increase so that the material will strengthen which is called the strain hardening which then the object will experience a form failure and break up [4]. Each initial load will experience elastic deformation to a condition with a certain value and experience a material failure, this is referred to as plastic deformation. The loading starts under the yield strength, causing the material to return to its original form due to the elastic nature of the material. The amount of material elasticity is largely determined by the modulus of elasticity. The modulus of elasticity can be calculated by finding the magnitude of the stress and divided

by the equation with the mathematical formula as follows:

$$E = \sigma / \epsilon \quad (6)$$

E = Modulus elastisitas

σ = Stress (MPa)

ϵ = Strain

Von-Mises (1913) states that the second yield deviator stress J_2 will exceed a certain critical value. Yield events occur when the distortion energy or shear strain energy of material reaches a certain critical value. So it can be said that the distortion energy is part of the total strain energy per unit volume involved in the deformation.

$$J_2 = k^2 \quad (7)$$

Von-Mises stress is used to estimate the rate of material weariness in a geometry against the loading conditions from the results of a simple uniaxial tensile test. Safety for the overall buckling structure is achieved by limiting the minimum buckling load factor to be greater than the user-specified safety factor. It is important to mention that the element is verified regarding the accuracy of the stress distribution by comparing it to established literature and solid elements [5].

2.2. Texture Design

The research of making a tsunami capsule prototype frame was carried out in the mechanical design laboratory of the Faculty of Engineering, the University of Jember with the sequence of steps in figure 1, the following are the steps in doing so:

- a. Drafting and determining the strain of the tsunami capsule geometry, there are 3 safety capsule concepts, namely the spherical shape shown in figure 2a with 3 reinforcement rods made of stainless steel, spherical shape with a diameter of 2 meters. The simulation results from the normal direction loading of 240 kg in the form of a maximum strain occur in the passenger seating area with a value of 0.461313 mm. Figure 2b ball shape with 6 reinforcement rods made of stainless steel with a diameter of 4 meters. The results of strain simulation on the passenger seat connection area with a value of 0.238 mm.

Figure 2b ovoid 6 stainless steel reinforcing rod 2 meters in diameter and 3 meters high. Simulation results of the frame strain in the second concept are located at the location of the connection of seating to the frame of 0.248454 mm. From the development of the outer shape of the capsule dimension, it turns out that the critical point that occurs is in the passenger seat so that the amplifier is searched for the frame.

- b. Selection of concepts from the overall form. From the simulation results, the ideal shape is an ovoid shape that has the smallest strain that occurs in the passenger seat of a tsunami capsule. The drafting of a tsunami capsule base amplifier frame is shown in figure 3-13, with various amplifiers based on the symmetry axis of the rectangular, triangle, and hexagon shapes. The shape of the reference frame is square with a size of 500 mm x 500 mm.
- c. An inventory of stress-strain concepts is shown in table 1 as a result of loading weighing 60 kg.
- d. The choice of a concept is based on the results of the lowest strain stress and the lowest simulation error rate.
- e. The discussion is shown in figure 14-17 which discusses the change in the value of strain stress to the provision of amplifiers in the tsunami capsule seat frame.



Figure 1. Research Methods

3. RESULTS AND DISCUSSION

By using octahedral elements, the selection of concepts in figure 2 with consideration of the principal stress parameters, the change in final length after loading and Von-Mises stress, then determined according to the best order is concept 1 of figure 2b, concept 2 of figure 2c, and Reference of figure 2a. From these results, it was further found that the critical area was in the section of the tsunami capsule passenger seat.

Making the concept of a tsunami base capsule base frame tsunami has 10 concept development analyzed using an octahedral element by giving a load weighing 60 kg in a uniform load condition with a fixed pedestal. The ranking of the selection of the amplifier manufacturing concept shown in figure 3-13 is based on the variable principal stress, displacement, and Von-Mises stress and is inventoried in Table 1. Then the ranking of the best concepts is obtained so that the best amplifier concept is concept 6 which is proven by the low displacement, low low principal stress, and Von-Mises stress and the greater the modulus Elasticity. As for the stable concept, it can be observed in figure 14-17, namely concepts 3,4,5,6, and 9 with the acquisition of ranking 1 obtained concept 6 with principal stress of $3.05E + 06$ Mpa and strain 0.00725 mm.

Analysis of the reference concept shown in figure 3 shows that the location of the critical area occurs in the vertical and horizontal directions. Deflection (displacement) that occurs parabolic dish from the end of each side. Discussion of concepts is a comparison with previous concepts in sequence and finally will be concluded by comparing as a whole.

Concept-1 was developed as a solution to correct references by adding frame amplifiers in the vertical axis shown in figure 4. From the simulation results, the maximum deformation only occurs on the horizontal side experiencing an increase of 0.0242 mm in figure 4c, then the maximum principal stress has an increase of $0.59E + 6$ MPa which occurs at the end of the frame in figure 4b, while for the maximum Von-Mises stress it drops by $0.32E + 06$ MPa.

Concept-2 is shown in figure 5 by providing frame amplifiers on the vertical and horizontal axis, the results of the simulation of deformation formed by parabolic on all frames of figure 5a evenly, the maximum principal stress has decreased from concept 1 by $0.04E + 6$ MPa for its location based on the picture frame connection 5b, the resulting deflection has

decreased from concept-1 which is equal to 0.0009 mm in figure 5c while the maximum principal stress has decreased from $0.35E + 06$ MPa from concept-1 occurred in figure 5d.

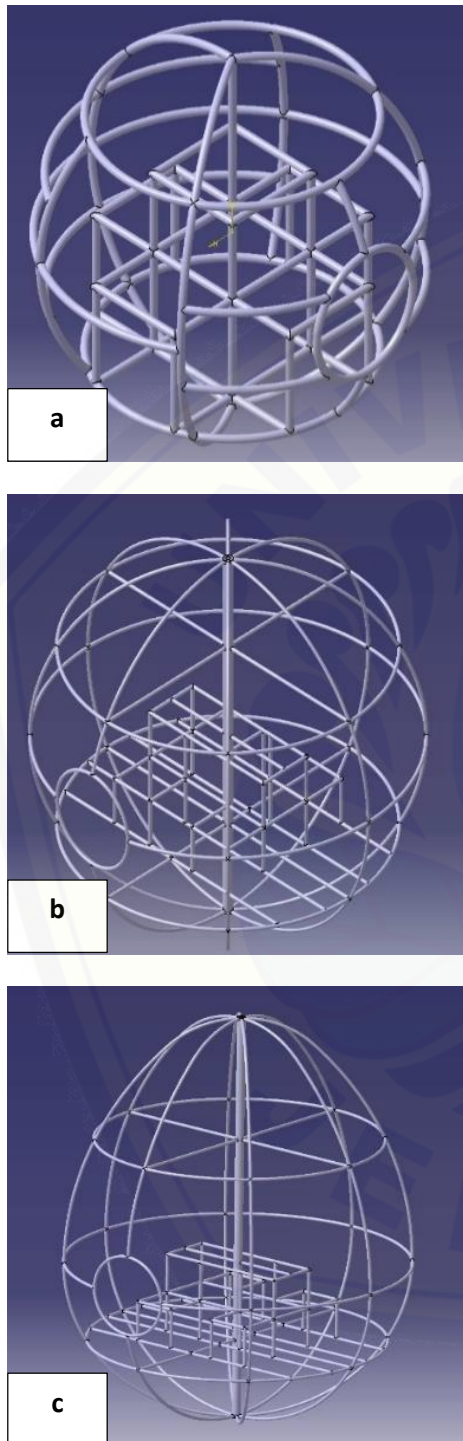


Figure 2. Geometrical Capsul Tsunami: a. Reference Concept, b. Concept-1, c. Concept-2.

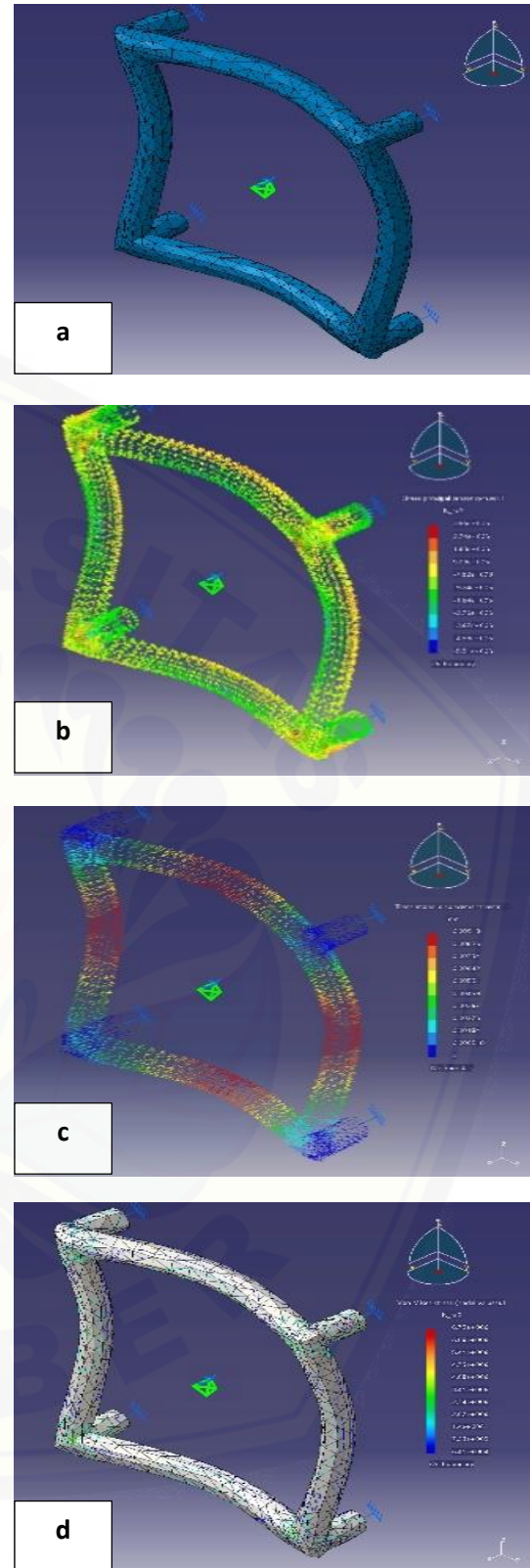


Figure 3. Frame Reference: a. Deformation, b. Principal Stress, c. Displacement (L_a), d. Von-Mises Stress.

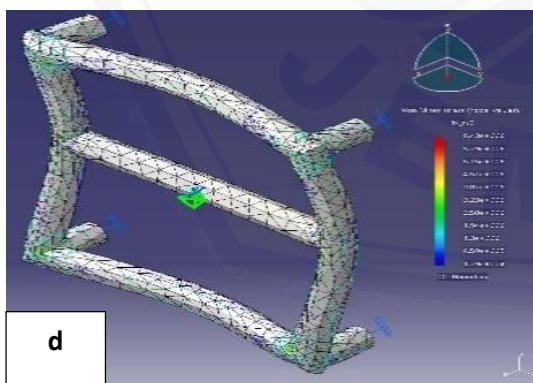
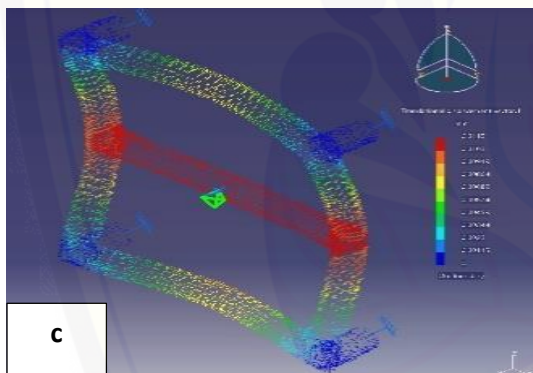
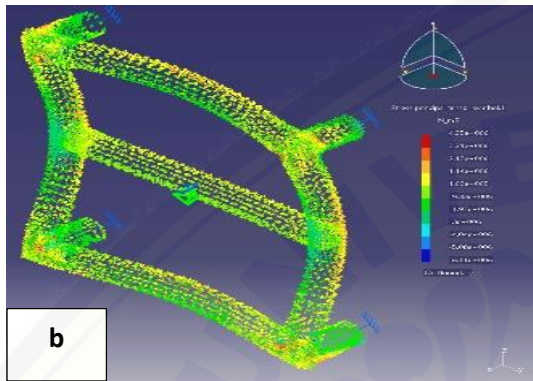
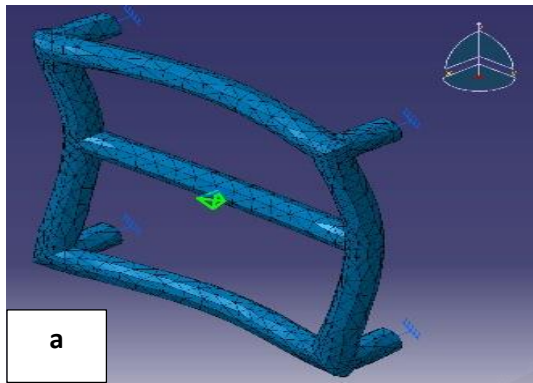


Figure 4. Concept Frame-1: a. Deformation, b. Principal Stress, c. Displacement (La), d. Von-Mises Stress.

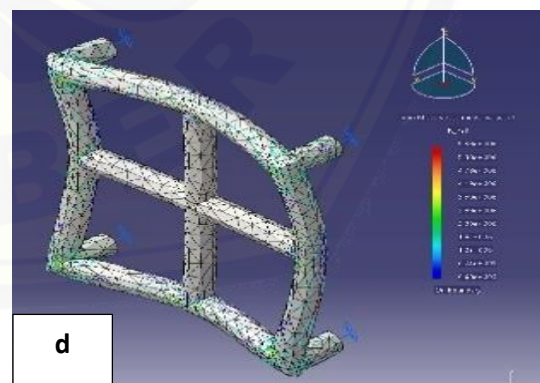
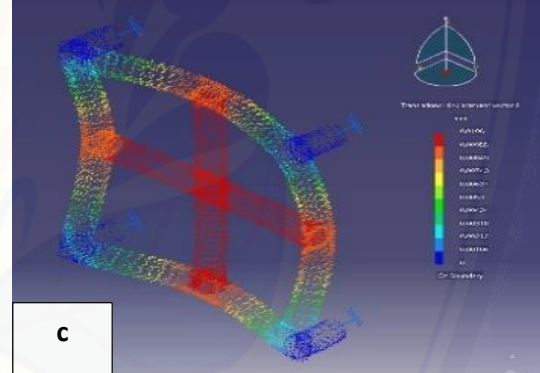
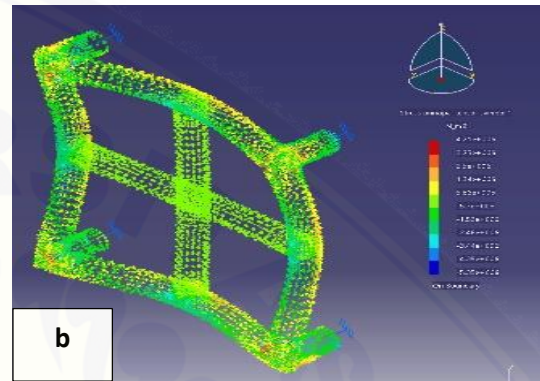
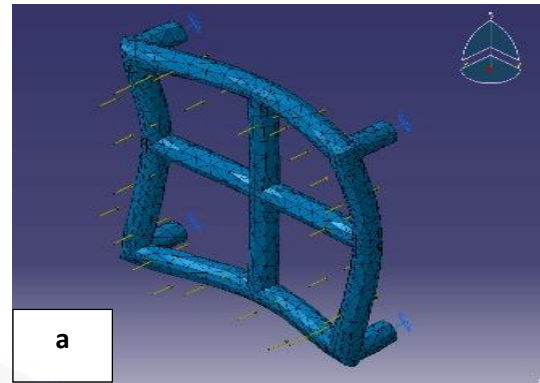


Figure 5. Concept Frame-2: a. Deformation, b. Principal Stress, c. Displacement (La), d. Von-Mises Stress.

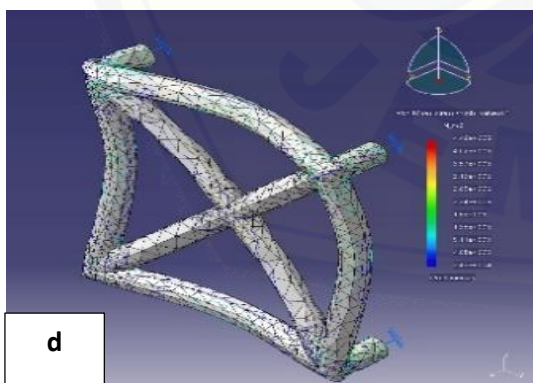
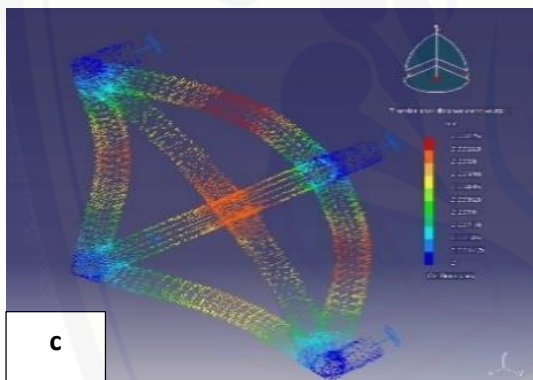
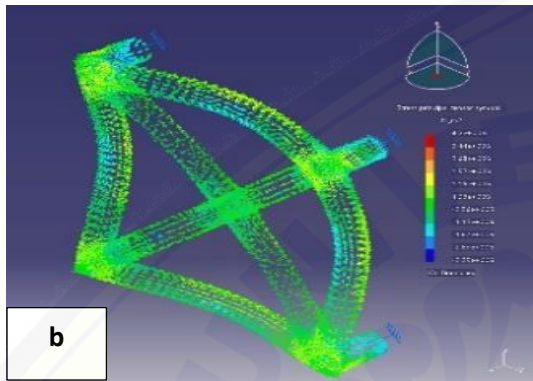
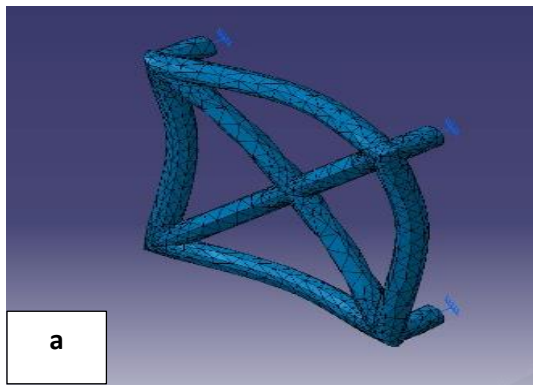


Figure 6. Concept Frame-3: a. Deformation, b. Principal Stress, c. Displacement (La), d. Von-Mises Stress.

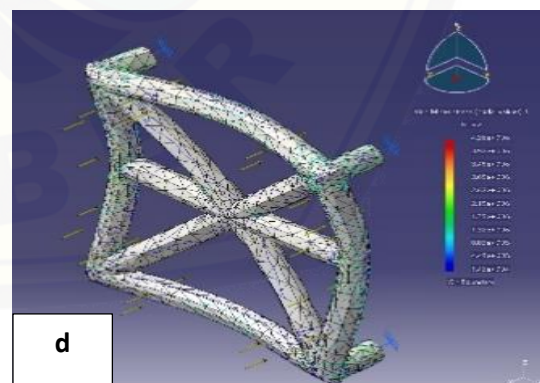
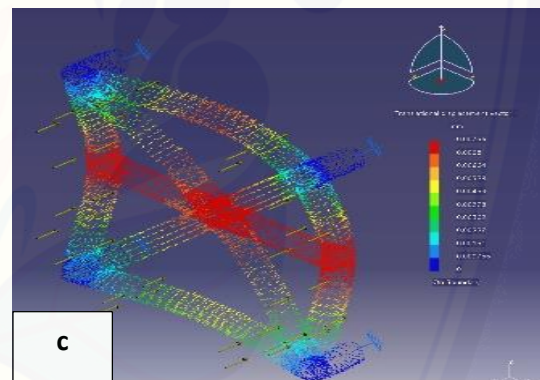
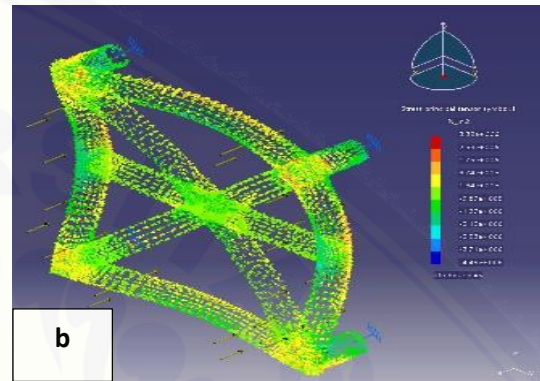
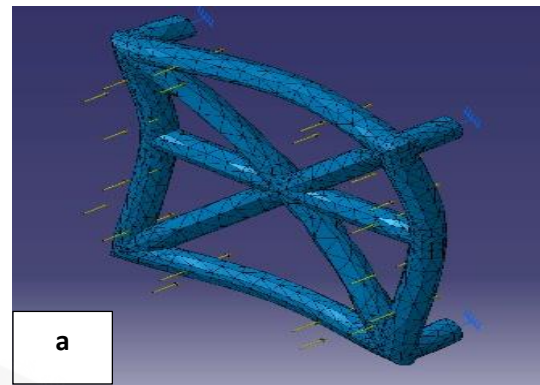


Figure 7. Concept Frame-4: a. Deformation, b. Principal Stress, c. Displacement (La), d. Von-Mises Stress.

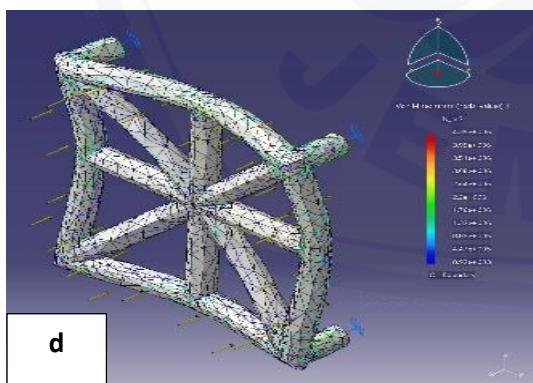
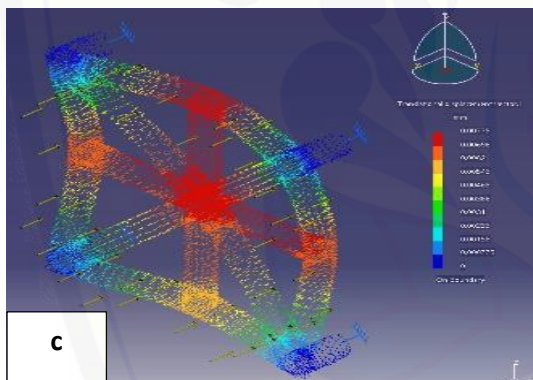
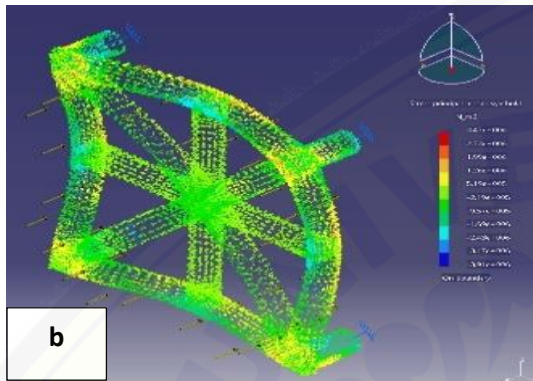
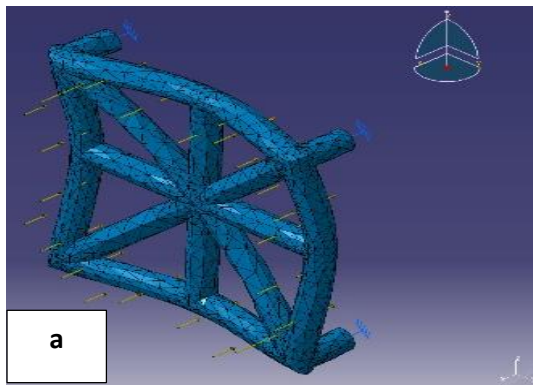


Figure 8. Concept Frame-5: a. Deformation, b. Principal Stress, c. Displacement (La), d. Von-Mises Stress.

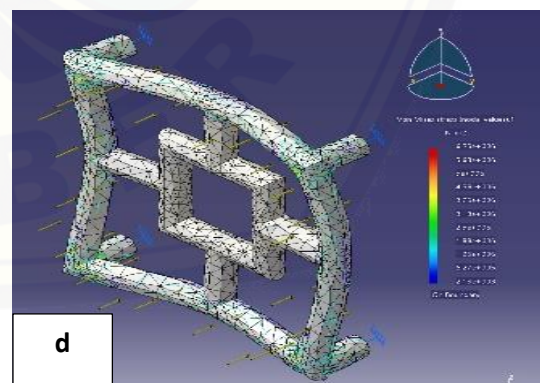
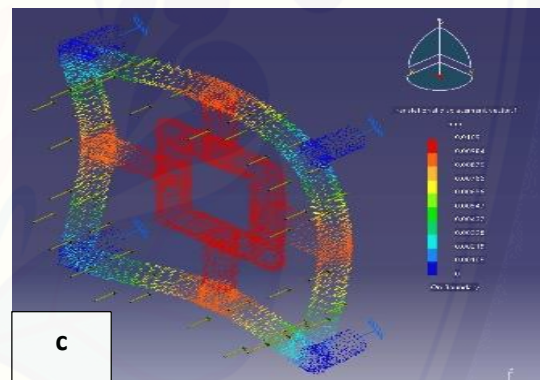
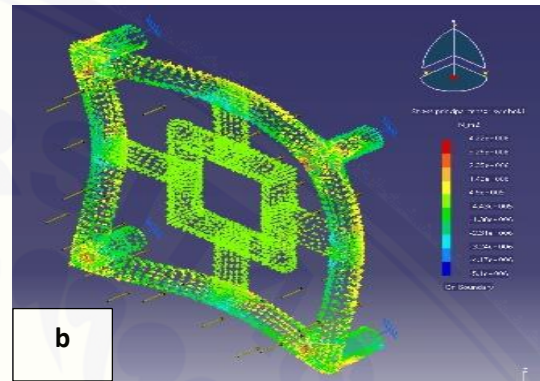
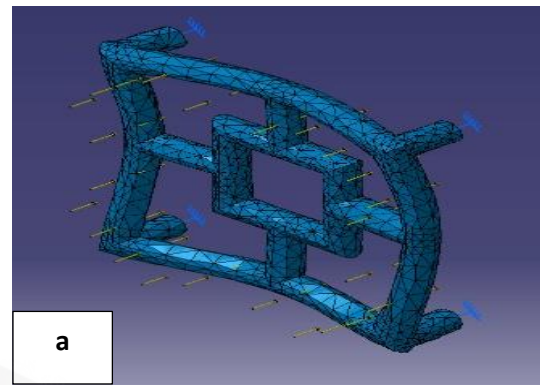


Figure 9. Concept Frame-6: a. Deformation, b. Principal Stress, c. Displacement (La), d. Von-Mises Stress.

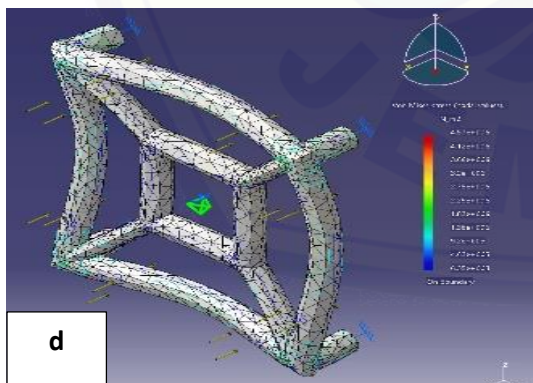
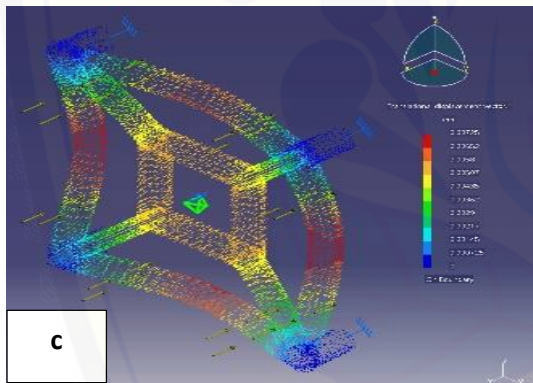
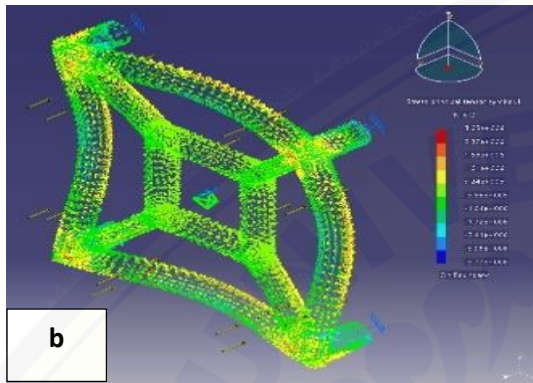
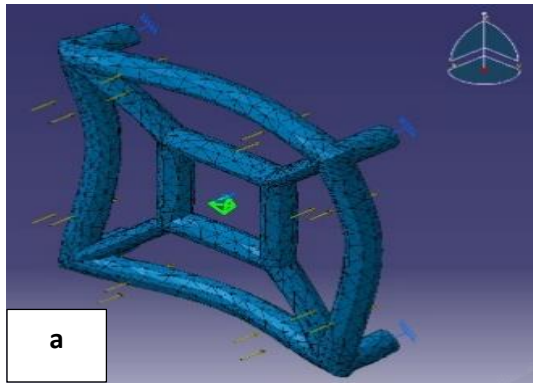


Figure 10. Concept Frame-7: a. Deformation, b. Principal Stress, c. Displacement (La), d. Von-Mises Stress.

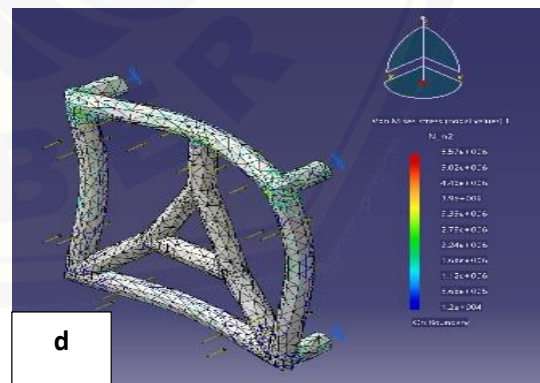
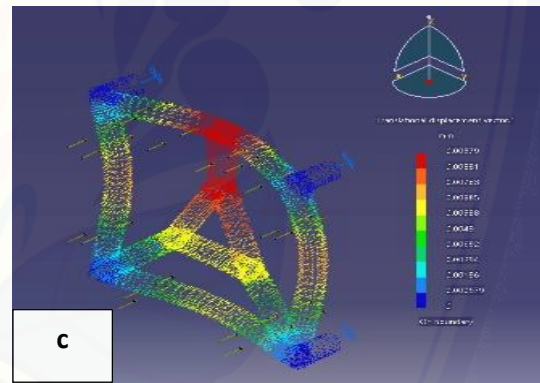
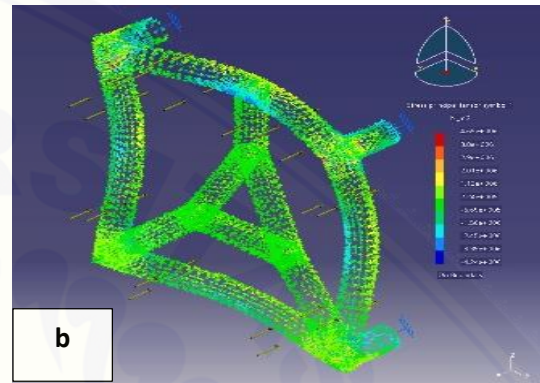
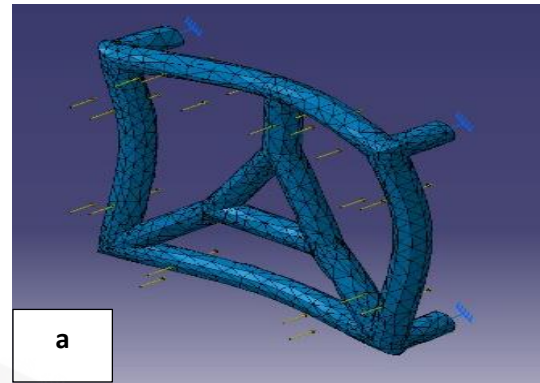


Figure 11. Concept Frame-8: a. Deformation, b. Principal Stress, c. Displacement (La), d. Von-Mises Stress.

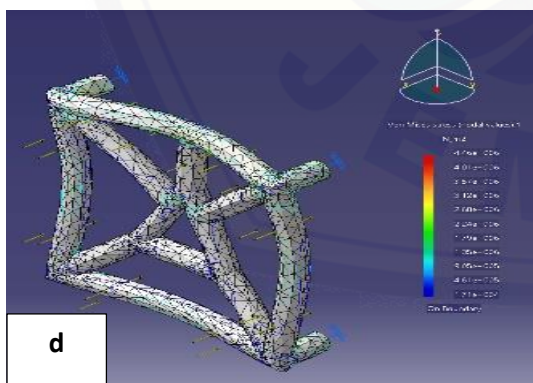
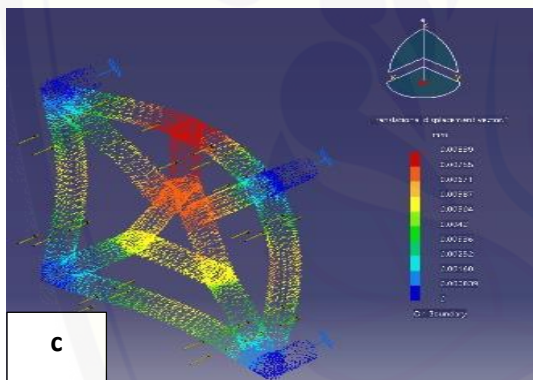
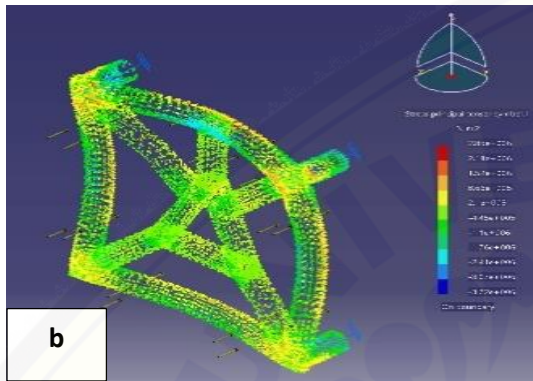
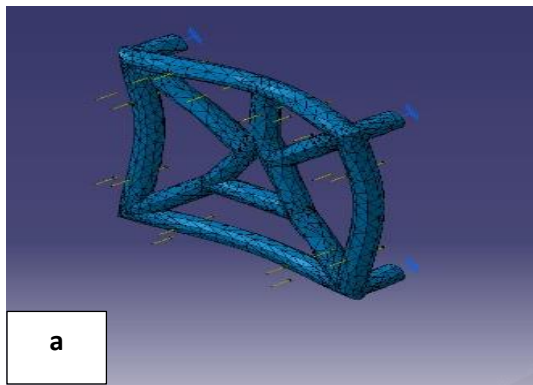


Figure 12. Concept Frame-9: a. Deformation, b. Principal Stress, c. Displacement (La), d. Von-Mises Stress.

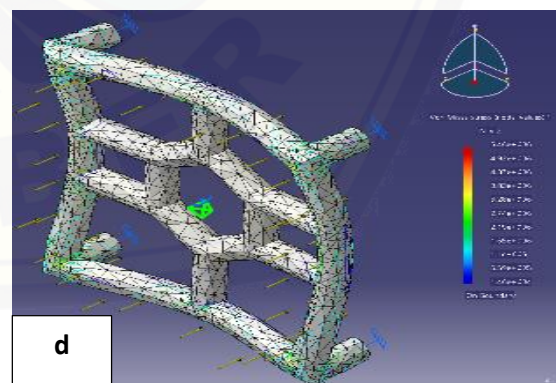
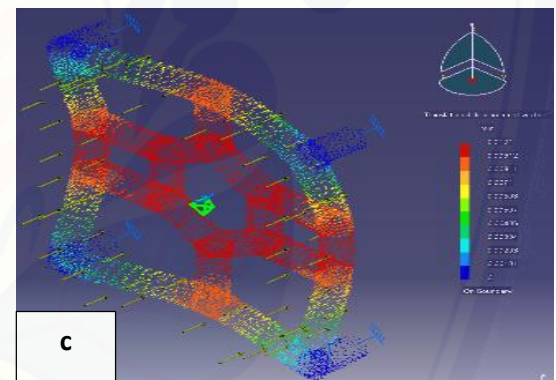
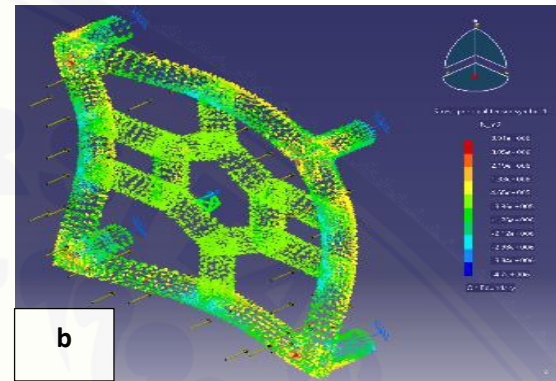
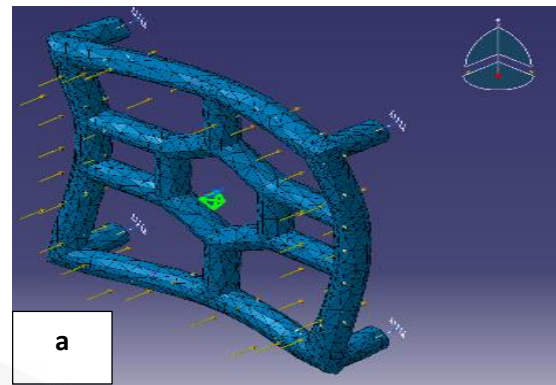


Figure 13. Concept Frame-10: a. Deformation, b. Principal Stress, c. Displacement (La), d. Von-Mises Stress.

Table 1. Ranking Concept Selection with 4 variables

Concept	Maks Principal Stress (MPa)	La-Lo (mm)	Maks Von-Mises Stress (MPa)	Estimation error	Modulus Elastic (MPa)	Ranking
Referensi	3.66E+06	0.00918	6.75E+06	8.47E-06	3.99E+08	9
Concept-1	4.25E+06	0.01150	6.43E+06	9.77E-06	3.70E+08	11
Concept-2	4.21E+06	0.01060	5.98E+06	8.18E-06	3.97E+08	8
Concept-3	4.20E+06	0.00725	4.46E+06	2.61E-06	5.79E+08	3
Concept-4	3.32E+06	0.00756	4.36E+06	2.36E-06	4.39E+08	2
Concept-5	3.47E+06	0.00775	4.39E+06	2.76E-06	4.48E+08	4
Concept-6	3.05E+06	0.00725	4.57E+06	2.13E-06	4.21E+08	1
Concept-7	4.22E+06	0.01090	6.25E+06	6.05E-06	3.87E+08	6
Concept-8	4.69E+06	0.00979	5.57E+06	8.47E-06	4.79E+08	5
Concept-9	2.83E+06	0.00839	4.46E+06	3.28E-06	3.37E+08	7
Concept-10	3.91E+06	0.01010	5.46E+06	6.47E-06	3.87E+08	10

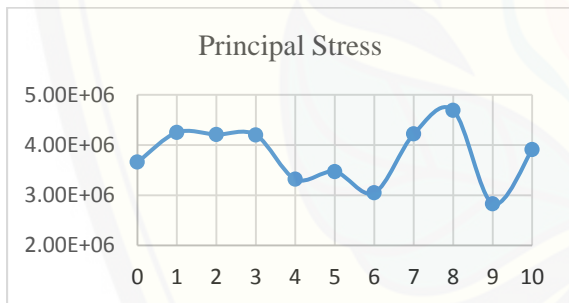


Figure 14. Principal Stress.

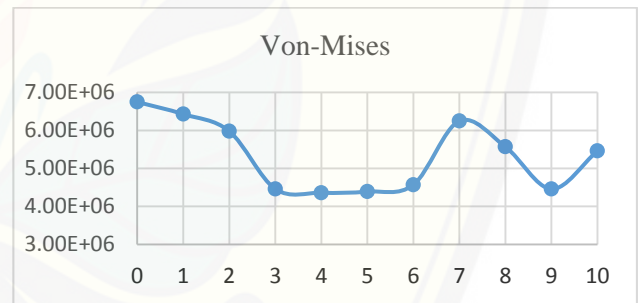


Figure 16. Von-Mises Stress.

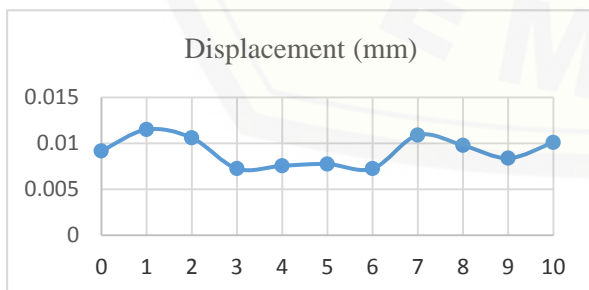


Figure 15. Displacement.

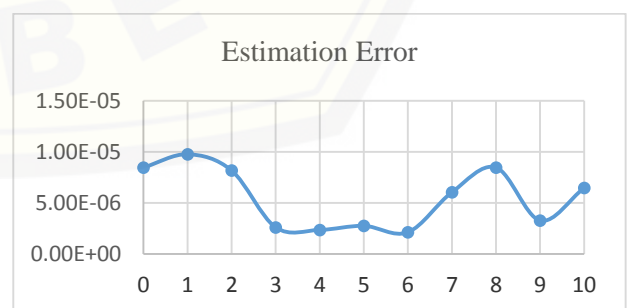


Figure 17. Estimation Error.

Concept-3 by adding an amplifier in the diagonal direction across the frame of figure 6a deformation produced by parabolic on the side, the maximum principal stress produced decreases by $0.98E + 06$ MPa in figure 6b, due to the administration of a diagonal direction amplifier which is too far away thus resulting in a deformation change of 0.00005 mm from concept-2, while the maximum Von-Mises stress has decreased by $0.52E + 06$ MPa.

Concept-4 is a joint development of concept-3 and concept 1 shown in figure 7a shows that the greatest parabolic deformation is experienced by the horizontal sides, the maximum principal stress has decreased from $0.28E + 06$ MPa, while for deformation has increased from concept 2 which is equal to 0.00031mm which is located on the horizontal side precisely on the flat diagonal side connection of figure 7b. For maximum Von-Mises stress, it decreases by $0.1E + 06$ MPa. The cause of deformation reduction in concept 4 is caused because the location of the amplifier is only given on the horizontal flat diagonal side only while vertical is absent.

Concept-5 is a desire to improve concept-4 by adding horizontal or vertical horizontal diagonal axis amplifiers. The reverse result is not as good as concept 4 and even becomes too bad in figure 8a shows that the center of gravity is concentrated in the central junction of the frame, the body blocks in the middle so that it causes the stress to increase the principal maximum of $0.15E + 06$ MPa with a change in color that was originally in concept 3 at the end of the blue connection now turns to green color in figure 8b, the maximum change in deformation increases of 0,00019 mm in figure 8c in the middle and vertical and horizontal ends of the joint, while for crossing diagonal connections there is no increase in deformation. The maximum Von-Mises stress rises to $0.03E + 06$ MPa from the concept 4 approved in the shaped.

Subject to the concept-5 increasing the clumping of the amplifier in the middle so the next concept-6 to try to dig up the clump with a square amplifier of 150 mm x 150 mm then in the middle a vertical and horizontal amplifier is provided which is connected to the frame in figure 9a, Principal stress is immediately asked if drastic $0.32E + 06$ MPa, the maximum deformation is also reduced by 0,00050 mm occurring along with the rectangular reinforcement and evenly distributed. The stress will reach a height increase of $0.46E + 06$ MPa at the position of the amplifier connection.

The concept-7 was developed by changing the concept-6 in the second part, namely the amplifier which was originally directed vertically and horizontally changed to diagonally crossed direction, the result is parabolic deformation evenly distributed on the side of the frame and amplifier as shown in figure 10a, the maximum principal stress occurs in the connection between the amplifier and the inner frame in figure 10b which has an increase of $0.117E + 06$ MPa, the maximum deformation has increased by 0.00365mm with an even distribution both in the frame and the figure 10c Von-Mises stress $1.68e + 06$ MPa in figure 10d connection area between amplifier and frame. The increase in all variables is caused by the ability of the diagonal crossing direction which can divide the loading evenly compared to concept-6 which concentrates on the square reinforcement section on the top of the frame.

Concept-8 by using an amplifier in the middle in the form of an equilateral triangle then in the taper section a straight amplifier is added to the frame shown in figure 11. Results in parabolic deformation on the horizontal side of the frame, the distance between the lower end and the lower end of the lower frame is longer than the end of the upper triangle to the center of the frame, this results in an increase in principal stress of $0.47E + 06$ MPa in figure 11b, for maximum deformation decreases by 0.00081 mm experienced by the amplifier of the

upper triangle tip 11c and the Von-Mises stress also decreases by $0.68E + 06$ MPa.

The concept-9 amplifiers is still an equilateral triangle but the addition of amplifiers is added to the diagonal cross at the top of concept-8 of figure 12a, the principal stress produced decreases $1.86E + 06$ MPa, the maximum deformation change decreases by 0.0014 mm, the Von-Mises stress also decreased $1.12E + 06$ MPa.

The concept-10 amplifiers use a hexagon shape then the outer taper end section is connected straight line to the picture frame 13. So that it forms a vertical and horizontal direction which is more numerous in the vertical direction resulting in parabolic deformation throughout the body frame. The maximum principal stress increased by $1.08E + 06$ MPa in figure 13b, the deformation change was 0.00171 mm and for Von-Mises the stress increased by $1E + 06$ MPa. Principal stress that occurs due to load on a geometrical concept, from the overall development of the concept of the principal stress results shown in figure 14 the value of the maximum principal stress with the value above the reference can be sorted from the largest value to the smallest value, namely the concept-8, 7, 1, 2, 3, and 10. While the value of the stress whose value is below the reference value from the largest value to the smallest value is the concept-5, 4, 6, and 9. Changes in distance or displacement experienced by a concept geometry are shown in figure 15, the displacement value of the concept is greater than the reference sequentially from the largest value of the concept 1, 2, 7 while the value is the same as the reference displacement of concept-8 and 10, and the values below the successive references of the concept-9, 5, 6, 4, and 3. Von-Mises stress as a level of material weariness in the geometry of various conceptual developments has been able to produce stress values under reference with the following concept -1, 7, 2, 10, 9, 6, 5, 4, and 3. Figure 16 is the level error in doing the simulation so that

it results in the accuracy of the calculation in all terms of the variable, the estimated error above the reference value is concept-1 while the values below the reference sequentially are concepts-8, 2, 10, 7, 9, 5, 4, 3, and 6. Figure 17 shows that the greater the error produced the wider the level of accuracy, so that it is determined that concept 6 has a high degree of accuracy. From the overall simulation results inventoried in table 1, then sorted according to the rank of the smallest value of the entire variable. The best results from the analysis conducted are concept-6.

4. CONCLUSION

Simulation results state that the selection of geometrical concepts with various shapes results in concept-1 which is a spherical shape with a diameter of 4 meters with a strength of 6 bars. **After** in the development of the concept or frame amplifier several things that affect the size of the simulation variable results in the form of a length of the amplifier, the position of the amplifier angle (vertical/horizontal/diagonal crosses), amplifier plane, the concept developer hopes can not only improve the condition of variables but can even reduce parameters in the results simulation variable. In this study, the geometry of tsunami capsules with 6 frame amplifiers was chosen using the concept-1 ball with a diameter of 4 meters, while the concept of reinforcing the passenger seat frame can still be applied, namely, the concepts-3, 4, 5, 6, and 9 because they have stability while those who will be selected using concept-6 because it has rank 1 in the selection of concepts.

5. ACKNOWLEDGMENTS

Authors are grateful to LP2M University of Jember that was funded this research in Academic Year 2019/2020.

REFERENCES

- [1] G.V. Nogueira, R.R. Paccola, H.B. Coda, A consistent UVLWT formulation for laminated plane frame analysis considering semi-rigid connections, *Finite Elements in Analysis and Design*, 2018; 140: 59-83.

- [2] T. Dang Hoang, C. Herbelot, A. Imad, N. Benseddiq, Numerical modeling for prediction of ductile fracture of bolted structure under tension shear loading, *Finite Elements in Analysis and Design*, 2013; 67: 56-65.
- [3] P. Aerias, T. Rabbcszuk, Steiner-point free edge cutting of tetrahedral meshes with applications in fracture, *Finite Elements in Analysis and Design*, 2017; 132: 27-41.
- [4] Navid Changizi, Mehdi Jalalpour, Topology optimization of steel frame structures with constraints on overall and individual member instabilities, *Finite Elements in Analysis and Design*, 2018; 141: 119-134.
- [5] Sascha Duczak, Fabian Duvingneau, Ulrich Gabbert, The finite cell method for tetrahedral meshes, *Finite Elements in Analysis and Design*, 2016; 121: 18-32.